All-Electron Nonempirical Calculations of Potential Surfaces. 4. Abstraction Reactions of Chlorine on Methane

Edwin L. Motell[1a] and William H. Fink* [1b]

Contribution from the Chemistry Department, California State University, San Francisco, California and the Department of Chemistry, University of California, Davis, California 95616. *Received November 7, 1975*

Abstract: Ab initio LCAO-MO-SCF and CI calculations in a Gaussian lobe basis set have been used to characterize the potential energy surface for the abstraction reactions of chlorine on methane. The three-center collinear reaction surface was first examined in the SCF approximation. The saddle point geometry of this surface was then taken to be that of the activated complex. The other degrees of internal freedom were than examined and parabolic fits to the calculated energies were used to determine harmonic force constants and minimum energy values for these degrees of freedom. CI calculations were then performed for the saddle point geometry and for the asymptotic limits of the surface. As expected for a reactin involving changes in the pairing of electrons, the thermochemical energies of reaction are badly miscalculated in the SCF approximation. The limited CI which was performed tended to correct the errors for the thermochemistry at the SCF level, but was not extensive enough to obtain satisfactory agreement with experimental values. Calculation of the kinetic isotope effect for the abstraction reactions of CH_2D_2 using the present results for the geometry and force constants of the activated complex produced comparable agreement with experiment as did a previous empirically chosen set of geometry and force constants. The large differences between these two potential energy surfaces suggest that there may be a wide range of geometries and force constants which result in agreement with experimental values for the kinetic isotope effect.

The general question of chemical reactivity has been addressed by generations of researchers and continues to be an area of great activity. Advancements in molecular beam techniques and the rapidly expanding knowledge of specific reaction cross sections have added impressive sophistication to the possibilities for the understanding of reactivity provided by more conventional kinetic studies. Theoretical developments[2] in chemical dynamics both in terms of classical trajectory studies[3] and nonclassical treatments[4] enable the calculation of reaction cross sections and kinetic rates from assumed potential energy surfaces. Quantum chemistry has advanced to the state of being in a position to offer valuable information about potential energy surfaces by enabling their calculation at selected points of the molecular geometries.[5] Much of the effort at understanding reactivity has focused on the reactions of halogens with hydrogen and hydrocarbons as being good representatives of chemically reactive systems both because of the importance of these reactions in themselves and as prototypes for other reactions. The present work is a quantum chemical study of the potential energy surface for the hydrogen abstraction reaction of chlorine atoms on methane.

The calculational methods applied in the present study are similar to those used in previously reported work[6] and will only be discussed briefly. All calculations are of the ab initio type employing a Gaussian lobe basis set.[7,8] The Hartree-Fock-Roothaan equations for the doublet system of methane and chlorine were solved by the orthogonally constrained method of Segal.[9] The configuration interaction calculations utilized an efficient four-index transformation procedure and a configuration interaction program developed locally.[10] The hydrogen abstraction reaction was initially treated as a three-center linear collision problem. The saddle point region on the Hartree-Fock surface for the rigid motion of H_3C-H-Cl was defined by performing a series of calculations for differing H_3C-H and H-Cl distances in this collinear arrangement. A point in the middle of this saddle point region was then chosn as representative of the activated complex and additional SCF calculations to characterize the potential energy surface for other degrees of freedom were then performed with this point as reference. The computing resources available precluded a complete optimization of all other degrees of freedom along the collinear points and also precluded CI calculations after the SCF for each point was calculated, but CI calculations were performed at the point representative of the activated complex and at the asymptotic limits of the surface, $\cdot CH_3$, HCl and CH_4, $\cdot$Cl.

Results

Table I presents the calculated SCF energies for the saddle point region of the linear hydrogen abstraction reaction and the asymptotic values of the surface. In all calculations except point 18, the other three hydrogens were retained fixed in the same positions they have for methane, namely HCH angle of 109°, R_{CH} = 2.06 a_0 (1.097 Å). Point 18 was obtained with a calculation on planar methyl radical with R_{CH} = 2.06 a_0.

Figure 1 is a contour diagram of the saddle point region, which can be inferred from the data of Table I. The contours in Figure 1 were constructed using a locally maintained version of the CALCOMP program GPCP, which ensures good local representation of the function being approximated. The center of the saddle point region was chosen to be at R_{CH} = 2.86 a_0 (1.513 Å) and R_{HCl} = 2.69 a_0 (1.423 Å) and best gradient axes for the saddle point were chosen as indicated, making included angles with the R_{CH} axis of 23°5′ and 62°0′. The first three points of intersection of the contours with these axes on both sides of the center were then used to least-square fit a parabola, thereby establishing the positive and negative curvatures of the saddle point. These curvatures could then be transformed into force constants and the mixing constant for the R_{CH},R_{HCl} motions of the activated complex.

Figure 2 represents the geometry of the activated complex and serves to label the degrees of internal freedom. The potential energy surface was investigated in the vicinity of the activated complex by applying distortions to the geometry obtained for the saddle point of Figure 1. The stretching constant $k_{CH'}$ was obtained by fitting a parabola to three points of a breathing mode distortion of the CH_3 group, including the saddle point geometry and one on either side of the saddle point geometry. The bending constant k_θ was obtained from a distortion which bent θ, but maintained the R_{CH} and R_{HCl} distances constant. The bending constant k_α and k_β and the minimum energy values of α and β were obtained from a total of four distortions about the saddle point and regarding the

Table I. Calculated SCF Energies

Point No.	R_{CH}[a]	R_{HCl}[a]	E[b]
1	3.10	2.36	−499.54715
2	2.90	2.56	−499.55207
3	2.70	2.56	−499.54956
4	2.70	2.76	−499.55484
5	2.50	2.96	−499.56590
6	2.30	3.16	−499.58288
7	3.10	2.56	−499.55483
8	2.90	2.76	−499.55158
9	3.10	2.76	−499.55039
10	2.90	2.96	−499.54587
11	3.50	2.36	−499.55607
12	3.30	2.56	−499.55766
13	3.10	2.96	−499.53965
14	3.30	2.76	−499.55061
15	3.50	2.56	−499.56023
16	2.86	2.69	−499.55280
17	2.06	∞	−499.6313
18[c]	∞	2.41	−499.5799

[a] Distance in Bohr radii (a_0). [b] Energies in Hartrees. [c] Methyl radical planar.

Table II. Force Constants and Geometry of the Activated Complex Found for the Ab Initio Surface

Constant	Calculated value[a]	Method
k_{CH}	-0.480×10^5	Interpolation on collinear surface
k_{HCl}	2.054×10^5	
k_{CHCl}	1.676×10^5	
$k_{CH'}$	7.761×10^5	Breathing mode distortion of CH_3 unit
k_θ	0.192×10^{-11}	Bending θ
k_α	0.754×10^{-11}	Four angular distortions
k_β	0.235×10^{-11}	
α_0	99.65°	
β_0	117.25°	
R_{CH}	1.513	Collinear search verified by breathing mode distortion of CH_3
$R_{CH'}$	1.097	
R_{HCl}	1.423	

[a] Stretching constants in dyn/cm, bending constants in erg/rad^2, distances in angstroms, angles in degrees.

resulting energies as a quadratic function of the deviation of the angles α and β from their minimum energy values. Table II summarizes the fore constants and minimum energy geometry found for the activated complex in this way.

The near thermochemical neutrality of this reaction has been well established ($\Delta H°(0\ K) = -1.2$ kcal/mol).[11] If this value of ΔH is corrected for the zero point vibrational energies of the species,[12-15] a value $\Delta E° = -5.8$ kcal/mol may be arrived at for the experimental value of the difference between the potential energies of ($CH_3\cdot$ + HCl) and (CH_4 + Cl·). One measure of the reliability of the calculated potential energy surfaces is to compare the differences in energy between the asymptotic limits of the surfaces with the thermochemical values for the same changes. These energy differences are among the most difficult quantities to obtain from a calculation, particularly, as in this reaction, when there are large changes in the pairing of electrons. Interelectron correlation energy differences become extremely important in these situations and although it was felt that an extensive attempt to include these correlation effects was inappropriate for the present investigation, since it was expected that correlation energies would be important for the asymptotic energy differences, a modest CI calculation was performed at these geometries in order to at least have a rough assessment of their importance.

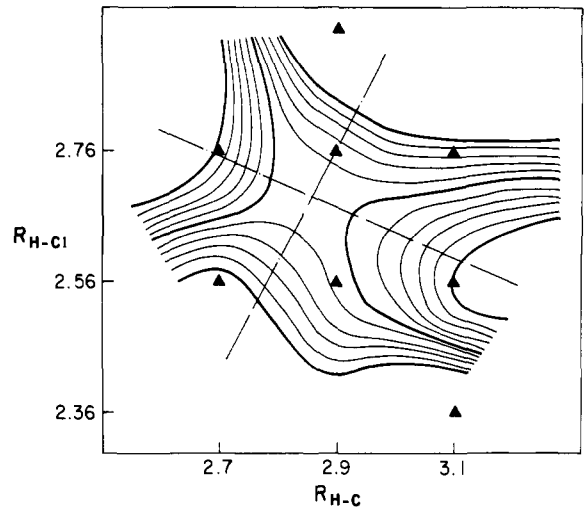

Figure 1. Contour diagram of the saddle point region of the calculated SCF surface. Filled triangles represent calculated points. The center lines define the chosen geometry of the activated complex and the directions for the natural axes of positive and negative curvature. The heavy line right uppermost represents an energy of −499.500 Hartrees. The heavy line left uppermost represents an energy of −499.550 Hartrees.

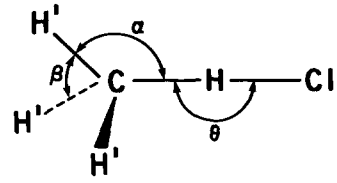

Figure 2. Geometric parameters for the reaction complex.

The configurations included in the CI were carefully chosen so as to treat both the asymptotes and the saddle point region equally. A careful consideration of possible excitations at the saddle point region and the correlation of these configurations into the asymptotes showed that a reasonably complete yet modest CI of 99 determinants at the saddle point region was possible. The configurations at the saddle point were obtained by taking all double excitations originating from the same orbital from the four highest occupied molecular orbitals to the lowest three virtual molecular orbitals, all single excitations from the three highest occupied to the lowest three virtuals, and by closing the open shell orbital by excitation from all of the valence orbitals lying below it. Following these configurations to their asymptotes shows that this choice of configurations is equivalent to choosing all symmetry allowed single and double excitations from ($1t_2$) to ($2t_2$, $3a_1$) in methane, from ($1e'$, $1a_2''$) to ($3a'$, $2e'$) in methyl radical, and from (2π, 5σ) to (6σ) in HCl. The SCF value for $\Delta E°$ for the reaction was 32.3 kcal/mol, the CI calculation result was 24.4 kcal/mol. Compared with the experimental value mentioned earlier of −5.8 kcal/mol, the calculations have very badly misrepresented the relative energies of the asymptotes. The CI calculation changes $\Delta E°$ by a large 8 kcal/mol in the sense to bring greater agreement with the experimental value, but still badly misrepresents the actual difference. Some comfort may be taken from the fact that the modest CI employed did indicate a large change in the thermochemical energy, o that it was at least able to warn that correlation energy differences were important.

One further comparison of the gross features of the calculated potential surface may be made with experiment. Figure 3 schematically depicts the reaction coordinate profile. The

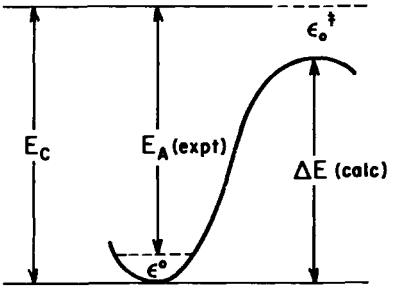

Figure 3. A schematic reaction profile demonstrating that E_c represents a quantity which may compare a completely experimental quantity with a completely theoretical one.

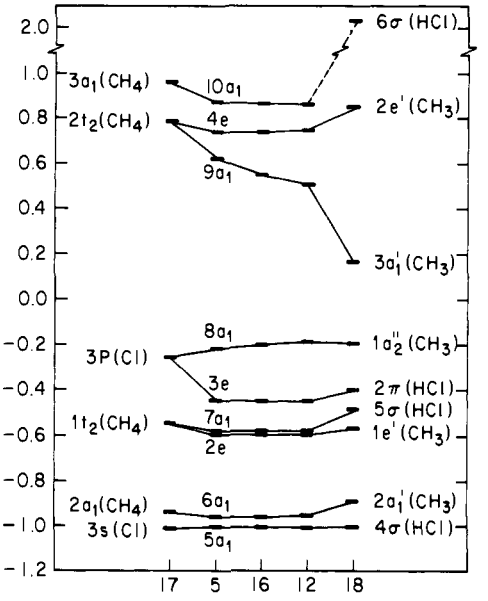

Figure 4. SCF one-electron energies at selected points across the reaction surface. These data show the smooth transformation of the orbitals within the SCF approximation from CH_4 + Cl on the left to CH_3 + HCl on the right. Because there is one unpaired electron throughout the reaction, a single configuration wave function is capable of correctly representing the changes in bonding which occur. The geometries of the selected points are given in Table I. Notice the break in the ordinate scale above 1.0 Hartrees.

experimentally determined activation energy is from the zero point energy of the reactants (ϵ_0) to the zero point energy of the activated complex ($\epsilon_0^{\ddagger}$). A comparison between a theoretical energy and an experimental energy is possible by adding the experimental zero point energy to the experimental activation energy[16] and by adding the calculated zero point energy of the activated complex to the calculated energy difference between reactants and activated complex. The zero point energy of the activated complex may be calculated by using the force constants, obtained for the surface and presented in Table II, in a normal mode calculation for the activated complex. Performing these calculations, one gets for the experimental value 26 kcal/mol, while for the theoretical value one gets 77.3 kcal/mol for the SCF calculation and 78.8 for the CI calculation. There is a disappointing discrepancy between the experimental and calculated values.

Despite the inability of the SCF calculations to quantitatively reproduce the experimental thermochemical energy differences between reactants and products, the qualitative nature of the changes in bonding are nicely accounted for. An examination of the details of the changes in one-electron energies and of the nature of the highest occupied molecular orbital as the reaction surface is traversed provides insight into the nature of the reaction and simultaneously identifies the origin of the quantitative deficiencies of the calculations. Figure 4 displays the one-electron energies calculated at selected points across the reaction surface. The numbers labeling the points along the abscissa correspond with the numbering of the points in Table I and serve to identify the geometry and total energy of the data being displayed. Figure 4 is then the calculated correlation diagram between the reactants CH_4 and Cl on the left and the products CH_3 and HCl on the right. Only the valence shell orbital energies are shown. The triply degenerate t_2 levels of CH_4 and the 3p orbitals of Cl are split as the Cl approaches along one of C–H bond axes into a doubly degenerate e set and a nondegenerate a_1. These degeneracies are unchanged upon further correlation to products.

During the course of the reaction, the orbitals are occupied through the $8a_1$ orbital, which is singly occupied. The character of this orbital undergoes the most severe change starting on the left as a chlorine p orbital, gaining C and H character as it loses Cl p character as the reaction proceeds. It ends on the right as the singly occupied $1a_2''$ orbital of methyl radical. These changes are shown in Table III, where the atomic orbital expansion coefficients for this orbital are displayed for the same gometries for which the one-electron energies are plotted in Figure 4. The gradual evolution of the orbital's character from Cl 3p to methyl radical is easily seen in these data. Analysis of the correlation diagram in Figure 4 permits interpretation of the changes in bonding as the reaction surface is traversed. Through the change in character of the $8a_1$ orbital the SCF wave function is able to describe the changes in electron occupation which occur during the reaction. The formation of the σ bond between the methane hydrogen and the chlorine atom is accommodated by the $7a_1$ orbital. It originates from the t_2 bonding orbital of methane and gradually evolves into the 5σ orbital of HCl.

Since the changes in character of the $7a_1$ and $8a_1$ orbitals correctly describe the changes in bonding and orbital occupation as the reaction surface is traversed, it is curious that the thermochemistry has been so badly misrepresented in these calculations. The resolution of the paradox becomes evident if we compare the calculated bond energies of CH_4 and HCl in the SCF approximation. The calculated energy difference between CH_4 and CH_3 + H is 0.13 Hartrees or 82 kcal/mol, which compares reasonably favorably with the experimental value of 101 kcal/mol. On the other hand the calculated energy difference between HCl and H + Cl is 0.083 Hartrees or 52 kcal/mol, which differs by 50 kcal/mol from the experimental value of 102 kcal/mol. We then see quite clearly that the deficiencies in the calculation of the thermochemical quantities for the reaction are almost entirely due to the failure of the SCF calculation to yield an accurate value for the bond energy of HCl.

Petke and Whitten[17] have reported a systematic study of the bonding in HCl and the influence of changes of basis set size and configuration interaction on calculated molecular properties. They concluded that the addition of d functions to the basis set was important to improve both the bond energy and one-electron properties, whereas configuration interaction had a major effect only on the energy. Because deficiencies in the present calculations appear to be in describing the HCl bond, similar improvements could be inferred for the present problem.

Kinetic Isotope Effect

To complete the examination of the calculated potential energy surface, the transition state region needs to be considered. The available experimental data, which provide a great amount of information about this region of the potential surface, are the changes of kinetic rates with various isotopically

Table III [a]

Atomic orbital	Cl Atom	5	16	12	Methyl[b]
$S_1(C)$		−0.00221	−0.00282	−0.00307	−0.00326
$S_2(C)$		0.24612	0.31554	0.33889	0.35058
$S_3(C)$		−0.04520	−0.05765	−0.06278	−0.06694
$P_x(C)$		0.	0.	0.	0.
$P_y(C)$		0.	0.	0.	0.
$P_z(C)$		0.61889	0.80125	0.88876	0.92872
H_1		0.12074	0.04381	−0.00575	0.
H_2		−0.06061	−0.07054	−0.07535	−0.07465
H_3		−0.06061	−0.07054	−0.07535	−0.07465
H_4		−0.06061	−0.07054	−0.07535	−0.07465
$S_1(Cl)$		−0.00008	−0.00069	−0.00005	
$S_2(Cl)$		−0.00257	−0.00237	−0.00162	
$S_3(Cl)$		−0.00731	−0.00638	−0.00421	
$S_4(Cl)$		0.01359	0.01078	0.00662	
$S_5(Cl)$		0.03192	0.03264	0.02343	
$S_6(Cl)$		−0.09977	−0.09561	−0.06446	
$P_x(Cl)$		0.	0.	0.	
$P_y(Cl)$		0.	0.	0.	
$P_z(Cl)$	−0.02643	−0.02216	−0.01673	−0.01136	
$P_x'(Cl)$		0.	0.	0.	
$P_y'(Cl)$		0.	0.	0.	
$P_z'(Cl)$	−0.26832	−0.23743	−0.17990	−0.12236	
$P_x''(Cl)$		0.	0.	0.	
$P_y''(Cl)$		0.	0.	0.	
$P_z''(Cl)$	1.03782	0.88098	0.67050	0.45486	

[a] The highest occupied molecular orbital (singly occupied) at selected points across the reaction surface. The geometries of the selected intermediate points are given in Table I. [b] Methyl radical in the pyramidal geometry obtained by removing one hydrogen from methane. The equilibrium geometry is of course planar and the singly occupied orbital in this basis set would then be a pure $P_z(C)$ orbital.

substituted methanes. The assumption of transition state theory for chemical reactions leads to the expression for the ratio of rate constants for two differently isotopically substituted sets of reactions on the same potential energy surface[18] of

$$\frac{k_1}{k_2} = \frac{\nu_1^*}{\nu_2^*} \pi \left(\frac{\Gamma_1}{\Gamma_2}\right)_{\ddagger} \pi \left(\frac{\Gamma_2}{\Gamma_1}\right)_r \left(\frac{\sigma_1}{\sigma_2}\right) \quad (1)$$

The ν^* are the imaginary frequencies of the reaction coordinate. The Γ's for the real frequencies are all of the form $\Gamma = u/2 \sinh (u/2)$; $u = h\nu/kT$; ν = the frequency of a normal mode. π implies a product over all normal modes of the species. σ_i is the chemical symmetry index of the reactants. The subscript $\ddagger$ refers to the activated complex and the subscript r refers to the reactant species.

Among the possible isotope effect ratios, there is experimental rate[19,20] data available for the following reactions:

$$CH_4 + Cl \rightarrow CH_3 + HCl \quad (I)$$

$$CD_4 + Cl \rightarrow CD_3 + DCl \quad (II)$$

$$D_2CH_2 + Cl \rightarrow D_2CH + HCl \quad (III)$$

$$H_2CD_2 + Cl \rightarrow H_2CD + DCl \quad (IV)$$

Of these the ratio k_{III}/k_{IV} would appear to be the more direct measure of the transition state region of the potential energy surface since in the expression (eq 1) all terms involving the reactants cancel. Table IV presents the harmonic frequencies calculated for the activated complex in each of the reactions I–IV, which were obtained from the standard G F matrix calculation using the force constants and geometry of Table II. The frequencies of Table IV in turn permit the calculation of the ratio of rate constants for reactions III and IV directly, which are presented in Table V. The fourth column of Table V would represent the tunnelling contribution to the kinetic isotope effect, assuming the calculated potential surface were a good characterization of the activated complex. The data in

Table IV. [a] Harmonic Frequencies for Activated Complexes

Symmetry designation	Reaction I	Reaction II	Reaction III[b]	Reaction IV[b]
e	3833.9	2861.9	2661.6	3709.7
			2862.6	3833.8
e	1518.16	1092.0	1046.1	1248.4
			1367.4	1295.5
e	1016.2	744.6	755.6	1002.1
			925.0	853.8
e	537.9	384.3	546.4	400.7
			430.3	450.0
a_1	3628.4	2576.3	3776.4	2754.8
a_1	1217.8	964.3	1483.7	1046.0
a_1	555.4	495.1	469.4	533.2
a_1	1821.0[c]	1335.6[c]	1820.4[c]	1337.3[c]

[a] Frequencies in cm^{-1}. [b] The e representation of C_{3v} splits into a' and a'' under C_s. [c] Imaginary frequency of the reaction coordinate.

Table V. Kinetic Isotope Effect for Reactions III and IV

T[a]	k_H/k_D (calcd)	k_H/k_D (expt)[b]	$\frac{k_H/k_D \text{ (expt)}}{k_H/k_D \text{ (calcd)}}$
250	11.61	14.4	1.24
273	9.53	12.1	1.27
325	6.76	8.2	1.21
344	6.12	7.1	1.16

[a] In kelvin units. [b] Reference 19.

Table V would suggest that for reactions III and IV, tunnelling is both small and about the same for both reactions and seems relatively temperature independent. This was the conclusion reached by Wiberg and Motell[20] using an empirically chosen force field and geometry for the activated complex. The differences between the previous empirical surface[20] and the

present ab initio surface would not have led one to expect such striking agreement with experiment for both calculations. The usual assumption of approximate equality of the two force constants k_{CH} and k_{HCl} being necessary to observe a high kinetic isotope effect is not met by the ab initio surface, but a high kinetic isotope effect is still calculated. A detailed look at the terms in eq 1 shows that the kinetic isotope factor originating from the symmetric stretch frequencies (469.4/533.2) is still nearly 1 in spite of the great difference between k_{CH} (-0.480×10^5) and k_{HCl} (2.054×10^5). These data suggest that a broad range of force constants and geometries may lead to similar results and that further investigation of the point is warranted.

The data of Table IV augmented with vibrational frequencies of the reactants also permits calculation of the kinetic isotope effect ratio for reactions I and II. The results of such calculations are not presented in detail because the calculated ratio was found to be extremey sensitive to the reactant vibrational frequencies used. If the direct experimental frequencies were used, the result at 303.7 K for k_I/k_{II} was 1.47 with very little temperature dependence. If the corrected harmonic frequencies were used the result was 2.95. When the frequencies for the activated complex derived from the empirically chosen force field and geometry[19] were used the result was 8.16 with the direct experimental frequencies of the reactants and 16.32 with the corrected harmonic frequencies.

Conclusion

While an ab initio calculation at this level of sophistication is not adequate for a quantitative calculation of the thermochemical energy differences for a reaction involving as severe changes in electronic structure as the present one, considerable qualitative understanding of the changes in bonding which occur during the reaction may still be derived. This is possible because the quantitative failings of the present calculations are contained almost entirely in the energy of the HCl bond at the asymptote of $HCl + \cdot CH_3$. The energies of distortion for the complex at the saddle point lead to force constants and resulting vibrational frequencies which are consistent with some of the observed experimental kinetic isotope effect data. However, because these force constants are very different from a previous empirically chosen set which were also consistent with the same experimental data, this agreement is weak evidence for the success of the calculations in describing the saddle point region of the potential energy surface.

Acknowledgment. We want to acknowledge the Research Corporation for their financial support. Ross Allardyce of Fireman's Fund American and Brian Beach were invaluable in assisting with the computations.

References and Notes

(1) (a) California State University; (b) University of California.
(2) No attempt at being complete in references to recent developments will be made; rather, selected references to work dealing with hydrogen abstraction reactions induced by halogens or hydrogen are included.
(3) (a) D. L. Bunker and M. D. Pattengill, *Chem. Phys. Lett.*, **4**, 315 (1969); *J. Chem. Phys.*, **53**, 3041 (1970); (b) T. Valencich and D. L. Bunker, *ibid.*, **61**, 21 (1974); (c) D. L. Thompson and D. R. McLaughlin, *ibid.*, **62**, 4284 (1975).
(4) (a) K. T. Tang and B. H. Choi, *J. Chem. Phys.*, **62**, 3642 (1975); (b) A. B. Elkowitz and R. E. Wyatt, *ibid.*, **62**, 2504 (1975); (c) W. H. Miller, *ibid.*, **61**, 1823 (1974); (d) M. Baer, U. Halavee, and A. Persky, *ibid.*, **61**, 5122 (1975).
(5) (a) K. Morokuma and R. E. Davis, *J. Am. Chem. Soc.*, **94**, 1060 (1972); (b) C. F. Bender, P. K. Pearson, S. V. O'Neill, and H. F. Schaefer, III, *J. Chem. Phys.*, **56**, 4626 (1972); (c) C. F. Bender, C. W. Bauschlicher, and H. F. Schaefer, III, *ibid.*, **60**, 3707 (1974).
(6) (a) W. H. Fink, *J. Am. Chem. Soc.*, **94**, 1073, 1079 (1972); (b) P. Pendergast and W. H. Fink, *ibid.* **98**, 648 (1976).
(7) J. L. Whitten, *J. Chem. Phys.*, **44**, 359 (1966).
(8) J. D. Petke, J. L. Whitten, and A. W. Douglas, *J. Chem. Phys.*, **51**, 256 (1969).
(9) G. A. Segal, *J. Chem. Phys.*, **53**, 360 (1970).
(10) P. Pendergast and W. H. Fink, *J. Comp. Phys.*, **14**, 286 (1974).
(11) "Selected Values of Chemical Thermodynamic Properties", *Natl. Bur. Stand. (U.S.), Circ.*, **No. 500** (1952).
(12) B. P. Stoicheff et al., *J. Chem. Phys.*, **20**, 498 (1952); J. Herrang and B. P. Stoicheff, *J. Mol. Spectrosc.*, **10**, 448 (1963).
(13) A. Snelson, *J. Phys. Chem.*, **74**, 537 (1970).
(14) H. M. Kaylor and A. H. Nielson, *J. Chem. Phys.*, **23**, 2139 (1955).
(15) G. Herzberg, "Molecular Spectra and Molecular Structure III. Electronic Spectra and Electronic Structure of Polyatomic Molecules", Van Nostrand, Princeton, N.J., 1967.
(16) A. F. Trotman-Dickenson and G. S. Milne, *Natl. Stand. Ref. Data Ser., Natl. Bur. Stand.*, **No. 9** (1967).
(17) J. D. Petke and J. L. Whitten, *J. Chem. Phys.*, **56**, 830 (1972).
(18) H. S. Johnston, "Gas Phase Reaction Rate Theory", Ronald Press, New York, N.Y., 1966.
(19) G. Chiltz et al., *J. Chem. Phys.*, **38**, 1053 (1963).
(20) K. B. Wiberg and E. L. Motell, *Tetrahedron*, **19**, 2009 (1963).
(21) H. S. Johnston and D. Rapp, *J. Am. Chem. Soc.*, **83**, 1 (1961).